

Early optical detection of cerebral edema in vivo

Laboratory investigation

*AMANDIP S. GILL, M.D., KIRAN F. RAJNEESH, M.D., M.S., CHRISTOPHER M. OWEN, M.D., JAMES YEH, MIKE HSU, M.S., AND DEVIN K. BINDER, M.D., PH.D.

Department of Neurological Surgery, University of California, Irvine, California

Object. Cerebral edema is a significant cause of morbidity and mortality in diverse disease states. Currently, the means to detect progressive cerebral edema in vivo includes the use of intracranial pressure (ICP) monitors and/or serial radiological studies. However, ICP measurements exhibit a high degree of variability, and ICP monitors detect edema only after it becomes sufficient to significantly raise ICP. The authors report the development of 2 distinct minimally invasive fiberoptic near-infrared (NIR) techniques able to directly detect early cerebral edema.

Methods. Cytotoxic brain edema was induced in adult CD1 mice via water intoxication by intraperitoneal water administration (30% body weight intraperitoneally). An implantable dual-fiberoptic probe was stereotactically placed into the cerebral cortex and connected to optical source and detector hardware. Optical sources consisted of either broadband halogen illumination or a single-wavelength NIR laser diode, and the detector was a sensitive NIR spectrometer or optical power meter. In one subset of animals, a left-sided craniectomy was performed to obtain cortical biopsies for water-content determination to verify cerebral edema. In another subset of animals, an ICP transducer was placed on the contralateral cortex, which was synchronized to a computer and time stamped.

Results. Using either broadband illumination with NIR spectroscopy or single-wavelength laser diode illumination with optical power meter detection, the authors detected a reduction in NIR optical reflectance during early cerebral edema. The time intervals between water injection (Time Point 0), optical trigger (defined as a 2-SD change in optical reflectance from baseline), and defined threshold ICP values of 10, 15 and 20 mm Hg were calculated. Reduction in NIR reflectance occurred significantly earlier than any of the ICP thresholds ($p < 0.001$). Saline-injected control mice exhibited a steady baseline optical signal. There was a significant correlation between reflectance change and tissue specific gravity of the cortical biopsies, further validating the dual-fiberoptic probe as a direct measure of cerebral edema.

Conclusions. Compared with traditional ICP monitoring, the aforementioned minimally invasive NIR techniques allow for the significantly earlier detection of cerebral edema, which may be of clinical utility in the identification and thus early treatment of cerebral edema. (DOI: 10.3171/2010.2.JNS091017)

KEY WORDS • absorption • aquaporin • astrocyte • edema • glia • laser • near-infrared • optics • scattering • swelling

CEREBRAL edema, an increase in brain tissue water content, is responsible for significant morbidity and mortality in many different disease states, including trauma, stroke, infection, tumor, and a host of chemical and metabolic intoxications. In fact, many patients with traumatic brain injury, worldwide the foremost cause of morbidity and mortality in persons under 45 years of age, experience a rise in ICP.^{11,16} Such increases in ICP can and often do lead to cerebral ischemia, herniation, and death.

Abbreviations used in this paper: FDPM = frequency domain photon migration; ICP = intracranial pressure; NIR = near-infrared; UCI = University of California at Irvine.

* Drs. Gill and Rajneesh contributed equally to the study.

Presently, there is no reliable technique to directly measure cerebral edema in vivo. This end point is currently assessed using ICP monitors, which employ a modality less than ideal for several reasons. First, these pressure transducers measure the physiological effects of cerebral edema rather than edema itself, which, due to the nonlinear compliance of brain tissue,¹² is an indirect and often imprecise surrogate of brain edema. Second, there is great variability in ICP depending on the cardiopulmonary cycle, head position, Valsalva maneuvers, and other physiological variables. Because of this practical limitation of real-time ICP monitoring, an empirical threshold of approximately 20 mm Hg has come to be defined as “pathological.”^{3,11} In most clinical settings, threshold detection of ICP elevation is what triggers clinical intervention. Therefore, at the

time of intervention cerebral edema has often already progressed significantly.

Because of these limitations, we aimed to develop a modality for detecting cerebral edema directly. Previous investigators have attempted to correlate other physiological variables to optical tissue properties, such as blood content, water content, and oxidation state.^{1,4,8,14,17,19,23,24} However, many of these techniques are highly invasive, impractical for clinical translation, and/or do not yield real-time data.

We reasoned that during the development of cytotoxic edema and the concomitant reduction of extracellular space volume, there should be a reduction in the scattering of NIR light through tissue with developing edema.^{4,13,24,28} Hence, a fiberoptic reflectance detector weighted toward the measurement of the scattering of light should theoretically allow for the direct detection of changes in light scattering associated with cellular swelling (cytotoxic edema). Here, we report the development of 2 distinct fiberoptic NIR techniques to monitor the reflectance of brain tissue *in vivo*. Using these systems in a mouse model of cytotoxic edema, we were able to detect the early development of cerebral edema significantly prior to a rise in ICP.

Methods

Fiberoptic NIR Spectroscopic Detection System

An implantable fiberoptic probe was created using two 180- μm core diameter quartz optical fibers (Ocean Optics), which were polished and bound together, separated only by their respective fiber cladding. One of these fibers (input end) was coupled to a stabilized 7-W tungsten halogen broadband NIR source and the other (output end) to a spectrometer coated for enhanced NIR spectral recording (Hamamatsu Photonics K.K./Zeiss, Inc.) (Fig. 1 upper). Data were recorded using LabVIEW (National Instruments) with a modified graphic user interface (Tec5USA). Reflectance values over the frequency range of 800–900 nm were integrated using 1-second sampling intervals.

Laser Diode-Optical Power Meter System

In these experiments, the source fiber of an identical dual-fiberoptic probe was coupled to an 850-nm diode laser via a collimator (TCLDM9, Thorlabs). The laser was driven by a laser diode power source (500-mA unit, Thorlabs) connected to a temperature controller (TED 200 C, Thorlabs). The detection fiber was connected to an optical power meter (PM 300, Thorlabs) for detection of NIR reflectance data, which were captured in real time using the PM 300 software (Thorlabs). The 850-nm laser was maintained at a constant temperature of 25°C and a constant current of 60 mA. The optical power meter was connected to a computer to record and store the data in a similar way as for the broadband system (Fig. 1 upper).

In a subset of experiments, a temperature probe (Model No. TSD202F, Biopac Systems) was placed adjacent to the dual-fiberoptic probe. The temperature probe was connected to a transducer and recorded continuously to computer (SKT100C, Biopac Systems). The power me-

ter recordings were time synchronized to temperature recordings. A baseline temperature was obtained before switching on the laser diode. The laser diode was turned on at 50 mA, and concurrent temperature and power meter readings were recorded for the same duration as the water intoxication experiments (see *Methods*).

We estimated the area of interrogation of the laser diode fiberoptic probe by using the look-ahead distance technique.¹⁸ Briefly, we used 7.5% agar solution and 4% intralipid phantom solution to ascertain the look-ahead distance using the solid-liquid interface changeover.

Correlation of Reflectance Probe Measurement With Optical Scattering Coefficient μ_s

To verify that our probe was weighted toward optical scattering, we used an FDPM system provided by the Beckman Laser Institute at UCI to determine the scattering coefficient, μ_s , at 850 nm of 4 intralipid phantoms (1, 2, 4, and 8%). We interrogated these phantoms with the fiberoptic probe to obtain reflectance values (Fig. 1 lower). Reflectance measurements were highly correlated with the FDPM-derived optical scattering coefficient, μ_s , at 850 nm ($r^2 = 0.9986$) ($p < 0.002$) (Fig. 1B).

Animals

All experiments were conducted using protocols approved by the UCI Institutional Animal Care and Use Committee. Adult 6–8-week-old CD1 mice were used in all experiments. The CD1 mice deficient in the glial water channel aquaporin-4 (AQP4 knockout mice) were also used as described below. These mice have normal growth, development, and maturation⁹ but have marked reduction in water flux across the blood-brain barrier in response to pathologic insults.^{10,26}

Surgical Technique

Mice were anesthetized (80 mg/kg ketamine/10 mg/kg xylazine) and immobilized in a stereotactic frame. Additional anesthetic was administered as needed to maintain an adequate level of anesthesia. After exposing the skull by midline incision, a high-speed drill (Drummond Scientific) was used to make a 0.6-mm right-sided bur hole 2 mm posterior and 2 mm lateral to the bregma. A custom-made dual-fiberoptic probe (see below) was positioned stereotactically to a depth of 1 mm (broadband system) or 150 μm (laser system) into the cerebral cortex. Care was taken to avoid torsion and flexion of the dual-fiberoptic probe. In a subset of animals (3 mice), an additional 0.6-mm left-sided bur hole was made with the identical anteroposterior and lateral coordinates to pass an ICP transducer (MPMS 100A-1 Micro Pressure Measurement System, Biopac Systems), which was synchronized to a computer and time stamped. In another subset of animals (6 mice), an atraumatic left-sided craniectomy was performed to obtain cortical biopsies (Fig. 2B). The craniectomy margins were the coronal suture anteriorly, the lambdoid suture posteriorly, and the attachment of the temporalis muscle laterally.

Water Intoxication Model

Cytotoxic brain edema from water intoxication was

Optical detection of cerebral edema

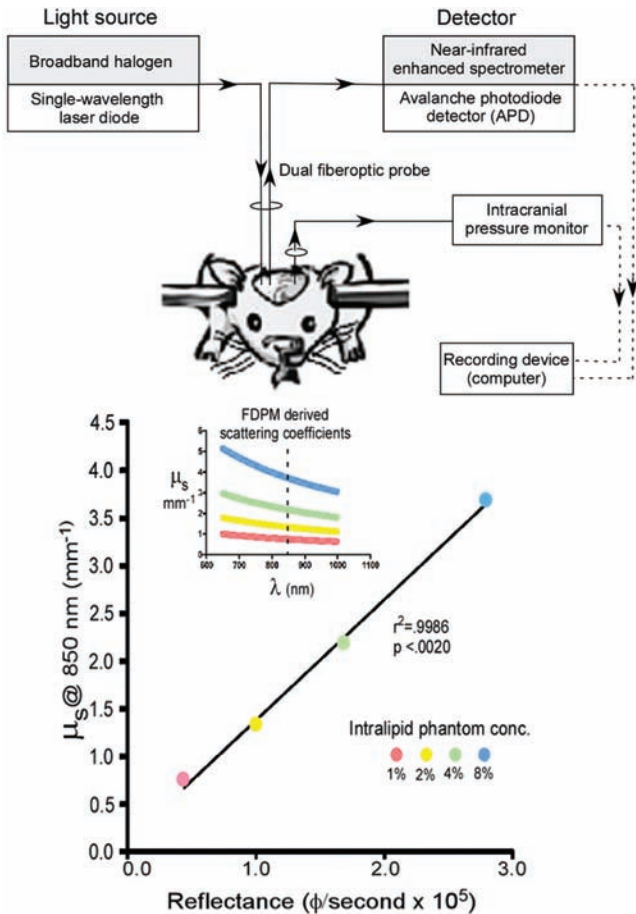


FIG. 1. In vivo dual fiberoptic probe assembly for detection of cerebral edema. Upper: The dual fiberoptic probe is implanted into the brain of the anesthetized mouse in a stereotaxic apparatus. One of the optical fibers is connected to the light source (broadband halogen or single-wavelength laser diode). The other optical fiber is connected to the detector apparatus (NIR-enhanced spectrometer or avalanche photodiode detector photometer). A mouse ICP monitor is implanted on the contralateral side for continuous measurement of ICP. Optical and ICP data are captured in real time and synchronized to a computer. Lower: Reflectance is correlated with optical scattering coefficient (μ_s). Frequency-domain photon migration experiments with intralipid phantoms (1, 2, 4, and 8%) were carried out to determine the correlation of optical reflectance measured by our fiberoptic probe and FDPM-derived scattering coefficients. Significant correlation between reflectance and scattering coefficient (μ_s) was observed ($r^2 = 0.9986$, $p < 0.002$). Inset shows the wavelength (λ , nm) $\times \mu_s$ (mm^{-1}) values derived from the FDPM instrument (see *Methods*).

produced in a similar way to that previously described.¹⁰ After baseline data were recorded for optical scattering and ICP, mice were injected with distilled water (30% body weight, intraperitoneally). In those animals in which cortical biopsies were taken, biopsies were obtained before and 15 and 30 minutes after water injection.

Analysis of Tissue Specific Gravity

Bromobenzene-Kerosene Gravimetry. Serial cortical biopsies were taken in a subset of mice (6 animals) to determine brain tissue specific gravity after injection of distilled water. A gravimetric density gradient column was

prepared as previously described^{5,12,15} with the following modifications: 1) a 250-ml graduated cylinder was used to mix the “heavy” and “light” solutions; 2) the heavy solution was made using 50 ml bromobenzene and 75 ml kerosene, while the light solution was made using 40 ml bromobenzene and 85 ml kerosene.

Eight NaCl solutions of known specific gravity were created using the Handbook of Chemistry and Physics, 57th edition,²⁷ to calibrate the column and generate a standard curve. These solutions were created by dissolving a known amount of NaCl into 50 ml of distilled water (Table 1). A droplet of each standard was placed into the column precisely over the surface. The position of the standard (midpoint) in the column was recorded 2 minutes later. This process was repeated for all NaCl standards, from which a standard curve (Fig. 2A) was constructed correlating specific gravity with position inside the cylinder. The equation generated was then used to calculate specific gravity of tissue biopsy samples placed in the column. New standard curves were generated before each experiment.

Cortical Biopsy Technique. Cortical biopsies were taken under a dissecting microscope (magnification $\times 10$, Olympus America Inc.) using 1-mm bronchoscopy forceps. Serial cortical biopsies were taken before (baseline) and 15 and 30 minutes after injection of distilled water (as described above) to establish baseline and changes in tissue specific gravity. Acquisition of optical data was suspended (Fig. 2C red bars) while the biopsies were performed due to saturation of the fiberoptic detector by light from the dissecting microscope and tissue movement around the fiberoptic probe. Immediately after the cortical biopsies were acquired, samples were placed in the column and the column position was recorded 2 minutes after sample placement. Tissue specific gravity was calculated using the equation generated from the standard curve.

Statistical Analysis

Baseline reflectance was defined following placement of probes and for at least 5 minutes prior to any experimental intervention. An “optical trigger” was defined as a decrease in reflectance by 2 SDs from baseline. Latencies from water injection to various ICP thresholds (10,

TABLE 1: Standard solutions for gravimetric column*

NaCl Concentration (g/50 ml)	Specific Gravity (g/cm ³)
2.5848	1.0354
2.8018	1.0386
3.1286	1.0434
3.4555	1.0482
3.6713	1.0513
4.1108	1.0577
4.5037	1.0635
5.0024	1.0707

* The NaCl concentrations are shown with their respective specific gravities for each of the 8 standard solutions.

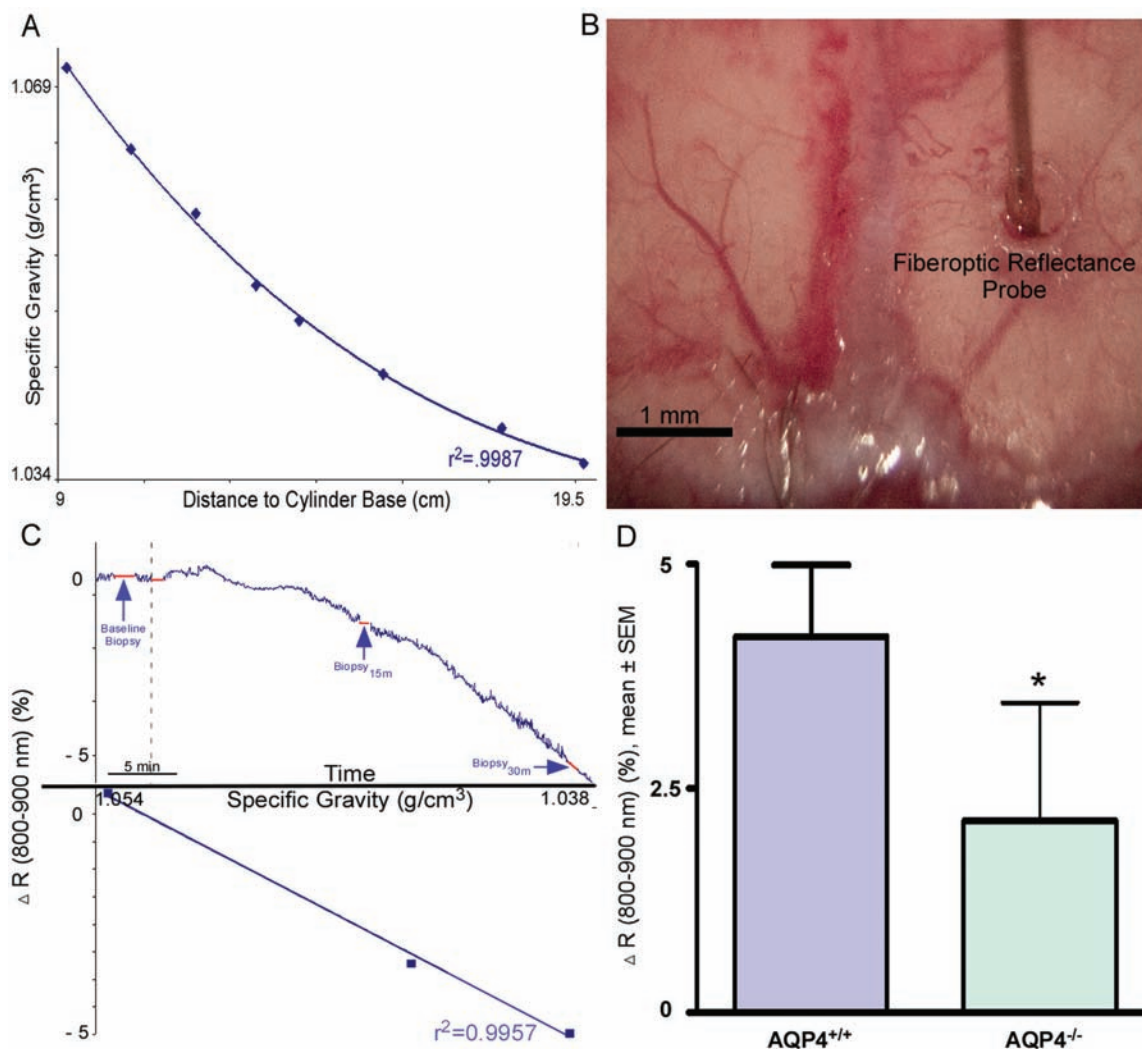


Fig. 2. Near-infrared optical reflectance is proportional to brain tissue water content. **A:** Standard curve constructed from the positions of the saline standards in the gravimetric column (see *Methods*). Specific gravities of cortical biopsies were then calculated using the equation generated from this curve. **B:** Exposure immediately prior to baseline biopsy via an atraumatic left-sided craniectomy. The dual-fiberoptic probe has been passed into the right cerebral cortex through a single bur hole. **C:** Near-infrared reflectance measurements obtained during acute water intoxication. Before and after injection of distilled water (30% body weight, intraperitoneally [dashed line]), serial cortical biopsies were obtained (baseline and at 15- and 30-minute time points [arrows]). Red bars indicate time periods during which data acquisition was suspended (see *Methods*). Upper: Note the sustained drop in reflectance following injection. Lower: A plot of reflectance versus tissue specific gravity in the same animal. Note that the reflectance is correlated to tissue specific gravity ($r^2 = 0.9957$ in this animal). **D:** Attenuated reflectance change in aquaporin-4 knockout (AQP4^{-/-}) mice. As in wild-type mice, in AQP4^{-/-} mice there was a linear relationship between reflectance and tissue specific gravity in all animals (3 animals [data not shown]; $r^2 = 0.983$). There was a statistically significant decrease in mean reflectance change (* $p < 0.05$) in AQP4^{-/-} mice compared with wild-type mice.

15, and 20 mm Hg) were calculated post hoc. Reflectance measurements were compared with gravimetric data using linear regression analyses, and reflectance measurements were compared with FDP-derivative scattering coefficients. We used a t-test to analyze scattering differences between wild-type and aquaporin-4 null mice. Intracranial pressure waveforms recorded at 10 Hz in Acknowledge software (Biopac Systems, Inc.) were postprocessed using the smoothing function with a mean of 10 values per second to derive second-long bins of mean ICP measurements and determine ICP cutoffs of 10, 15, and 20 mm Hg.

Results

Fiberoptic NIR Reflectance Correlates With Cortical Tissue Specific Gravity

To test whether our reflectance probe provides a direct measure of cerebral edema, fiberoptic NIR reflectance from 800–900 nm was measured while serial cortical biopsies for tissue specific gravity measurement were taken before and during water intoxication (Fig. 2B). We observed a consistent drop in reflectance following intraperitoneal injection of distilled water (Fig. 2C upper).

Optical detection of cerebral edema

There was a significant correlation between reflectance change and tissue specific gravity in this example (Fig. 2C lower), a relationship that held across all wild-type mice (3 animals [data not shown], $r^2 = 0.998$). Control animals showed no change in reflectance signal or tissue specific gravity after injection of saline (30% body weight, intraperitoneally) (2 animals [data not shown]).

To further validate this change in reflectance as that of a consequence of water intoxication, we repeated this experiment in AQP4^{-/-} mice. As stated, these mice lack the primary water transport channel of both human and mouse CNS, AQP4, which has been shown to result in impaired water transport across the brain.^{10,26} Once again, there was a correlation between changes in reflectance and tissue density in this subset of animals (3 mice; $r^2 = 0.983$). Interestingly, the magnitude of reflectance change in AQP4^{-/-} mice was significantly less ($p < 0.05$) than that of wild-type mice (Fig. 2D). Together with the previous experiments, this result indicates that our reflectance probe correlates with brain tissue specific gravity.

Fiberoptic NIR Monitoring Allows for Detection of Cerebral Edema Before ICP Increases

Broadband System. Having verified that our fiberoptic probe does measure cerebral edema, we compared our method with ICP measurement, the current clinical standard. In these experiments, an ICP transducer was placed through a bur hole into the left cerebral cortex (Fig. 3A). As before, after injection of water, we observed a progressive and sustained decrease in reflectance (Fig. 3B). This decrease occurred long before a rise in ICP. In fact, in this example, a significant change in reflectance (defined as a decrease in reflectance greater than 2 SDs from baseline) occurred 21.2 minutes before a pathologically increased ICP of 20 mm Hg was reached. On average, there was a significant change in scattering coefficient 27.9 minutes prior to ICP reaching 20 mm Hg, with a maximum lead time of 43.4 minutes. Summary data indicated that the optical trigger was consistently reached earlier following water injection than the ICP threshold values of 10, 15 and 20 mm Hg (3 animals) (Fig. 3C).

Laser Diode-Power Meter System. The aforementioned experiments determined that integration of NIR reflectance from 800 to 900 nm from a broadband source was useful for detecting cerebral edema. However, we noticed that, with our broadband source and with this integration technique, there was significant baseline variation in our optics setup. Therefore, we reasoned that a single-wavelength laser diode at 850 nm might provide a more stable NIR optical source, and we coupled this to a sensitive avalanche photodiode detector (optical power meter) (*Methods*). Using this system, we indeed observed much less baseline optical power variation and reflectance variation. As before, reduction in reflectance occurred early after water injection in all cases. In the example shown (Fig. 4A), the optical trigger (defined as a 2-SD reduction from baseline reflectance) occurred 31 minutes before the ICP monitor rose to 20 mm Hg. In these experiments, as the ICP rises, the variability of the ICP waveform increases (Fig. 4A insets). These observations were uniformly seen

in all animals (3 mice). In control mice injected with normal saline, ICP and the optical readings remained at baseline throughout the duration of the experiment (Fig. 4B) (representative of 3 control mice).

Thus, this laser diode-power meter system provided improved optical stability at baseline and detected cerebral edema in water-injected animals early in the course of brain swelling. In all mice (3 animals), the optical trigger occurred many minutes before the pathological rises in ICP to 10, 15, or 20 mm Hg ($p < 0.001$ compared with all 3 ICP thresholds) (Fig. 4C).

In addition, we observed no increase in brain temperature even following prolonged periods (> 2 hours) with the laser at 50 mA. At 50 mA of power (used in the water intoxication experiments), the look-ahead distance (defined in *Methods*) was determined to be 5 mm (Fig. 4D). We also determined that the power of the laser diode is linearly related to the look-ahead distance (Fig. 4D).

Discussion

We developed a novel fiberoptic NIR probe that provides direct measurement of cerebral edema through measurement of optical scattering. First, using intralipid phantoms, we found that reflectance measurements taken with the probe were highly correlated to optical scattering coefficient. Second, using bromobenzene-kerosene gravimetry of cortical biopsies, we established our fiberoptic NIR technique as a sensitive measure of brain edema. Third, we demonstrated reduced reflectance change in AQP4^{-/-} mice, which lack the primary glial water channel in the brain. Fourth, to establish this technique as a clinically relevant method, we were able to detect cerebral edema significantly prior to any change in ICP. Fifth, we optimized our source (850-nm NIR laser diode) and detector (sensitive avalanche photodiode detector) for even better optical stability and earlier detection.

Intracranial pressure monitoring is the current clinical standard for detecting cerebral edema but has several disadvantages. First, ICP monitors are susceptible to great baseline variability,³ often making the interpretation of absolute pressure and subsequent increases in pressure difficult. Second, as absolute pressure increases, signal variability increases (as shown also in our studies). Third, ICP waveforms fluctuate with changes in blood pressure, respiration, head position, exercise, and any types of Valsalva maneuver.³ However, the most significant disadvantage of ICP monitoring is the fact that due to the nonlinear compliance of brain tissue, significant edema can develop before ICP elevates.

In contrast, fiberoptic NIR detection allows for direct interrogation of cerebral tissue. The Mie theory predicts that the optical scattering coefficient varies with the size and concentration of scattering moieties. The most likely candidates for scattering moieties in the brain include mitochondria, other large organelles and proteins, and plasma membranes.^{20,22} Theoretically, as edema progresses, the distance between these organelles increases and thus the volumetric concentration of scatterers decreases. Our results indicate that reduction in optical scattering can be detected in real time. Near-infrared detection was previ-

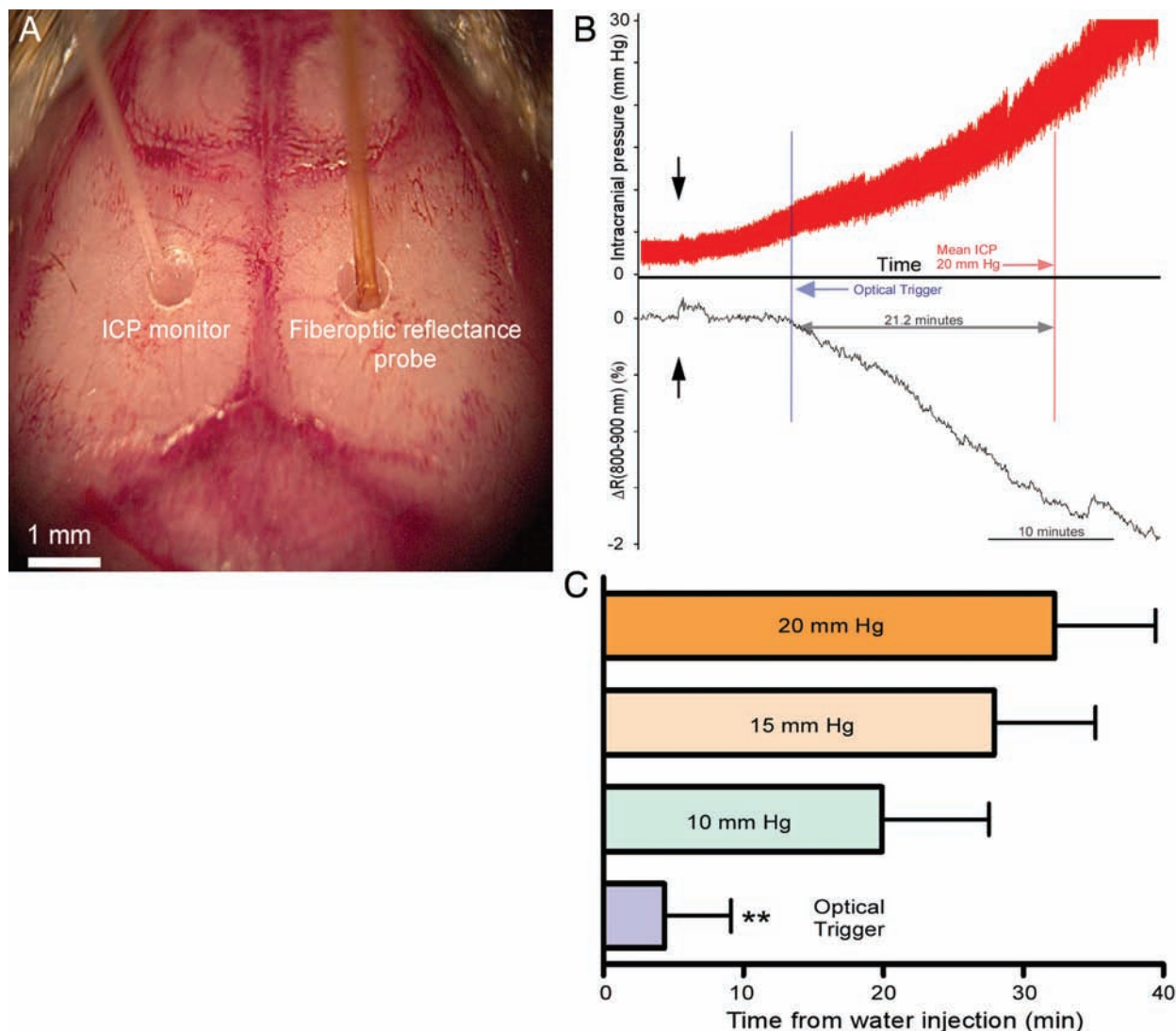


Fig. 3. Early detection of cerebral edema with a fiberoptic NIR system using a broadband halogen light source. **A:** A dual-fiberoptic probe is passed into the right cerebral cortex through a bur hole while the ICP monitor is placed contralaterally. **B:** Intracranial pressure measurements (upper portion of graph) before and after the injection of distilled water (30% body weight, intraperitoneally [black arrows]). Near-infrared reflectance measurements obtained with fiberoptic probe (lower portion of graph). In this example, the optical trigger (vertical blue line, for significant decline in baseline reflectance; see *Methods*) occurs 21.2 minutes prior to reaching a pathologically increased ICP of 20 mm Hg. **C:** Latency between injection of water (Time Point 0), optical trigger, and defined threshold ICP values (3 animals; mean \pm SEM). Optical trigger for a decline in reflectance occurs well before threshold rises in ICP to 10, 15, or 20 mm Hg. ** $p < 0.02$ compared with 10, 15, or 20 mm Hg.

ously employed in a pioneering study of cerebral edema,²⁴ which partially inspired our current study. In that study, NIR of 850-nm wavelength was used in mouse brain slices and in vivo through intact skull. The authors of that study found, similar to our current study but using different instrumentation, that during brain tissue swelling due to water intoxication there is an increase in NIR light transmittance (through brain slices), likely due to reduced scattering as in our current study. The changes in NIR signal were markedly attenuated in AQP4^{-/-} mice.²⁴

Fiberoptic tissue interrogation presents several technical challenges. Movement artifact and bleeding can produce optical data that cannot be interpreted. Therefore, we maintained rigid skull fixation and placed the probes away from blood vessels. Furthermore, significant

differences in scattering coefficient between gray and white matter necessitate consistent depth of probe placement. To eliminate probe torsion and microbending during brain swelling, we configured the bur hole diameter to precisely accommodate the diameter of the dual-fiberoptic probe. Due to the relatively small overall magnitude change in reflectance signal (approximately 2–10% from baseline), maintenance of stable source-detector fiber tip separation was crucial. We found that the distance between the optical probes was inversely related to optical reflectance (as expected by inverse square law [data not shown]). Lastly, we chose the 800–900-nm range because of the relatively low water and hemoglobin absorption coefficients at these wavelengths.⁶ This also accounts for the choice of the 850-nm single-wavelength laser diode. Fur-

Optical detection of cerebral edema

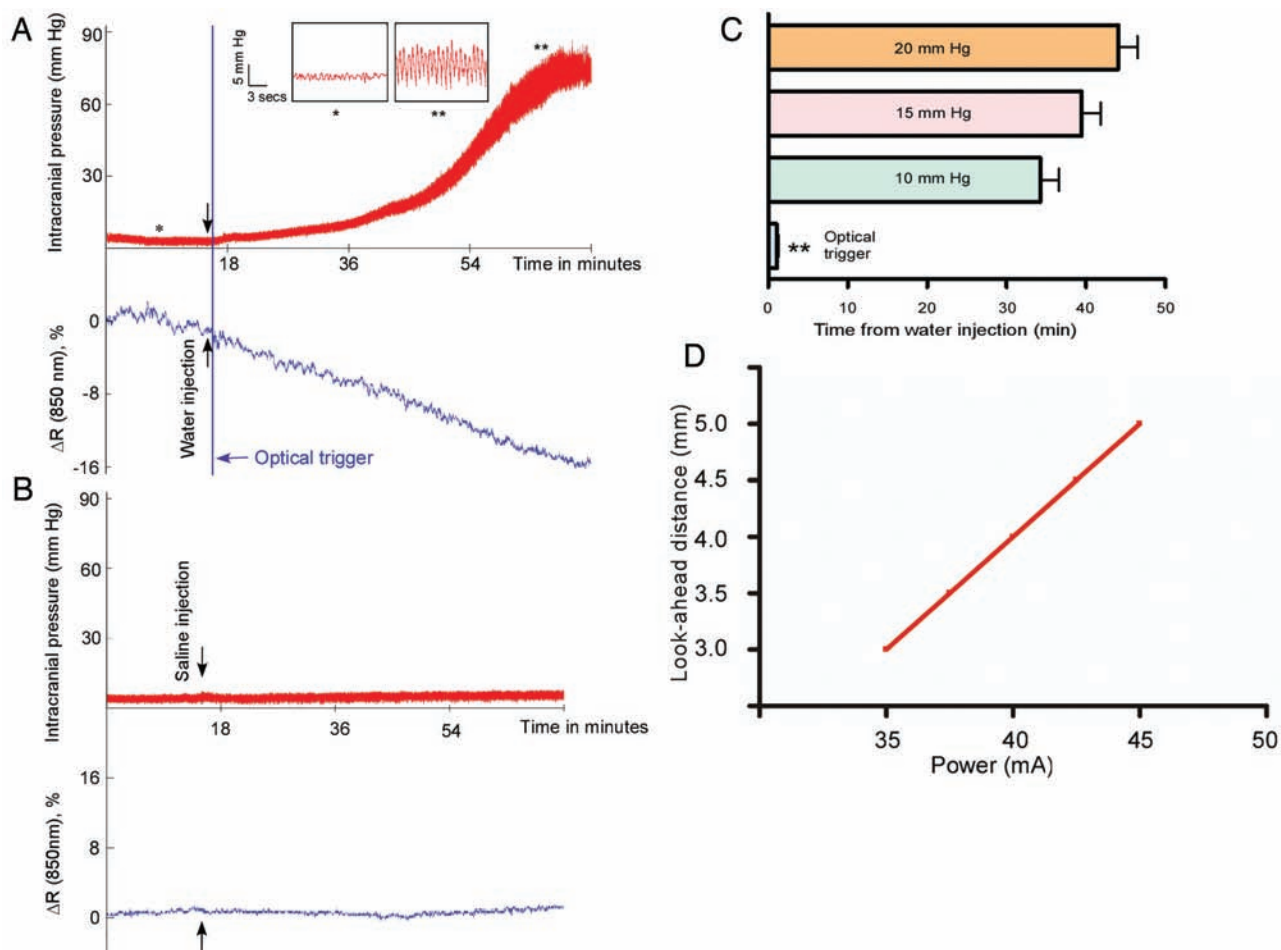


FIG. 4. Early detection of cerebral edema with a single-wavelength NIR laser diode-power meter system. **A:** Intracranial pressure recordings (upper portion of graph) before and after the injection of distilled water (30% body weight intraperitoneally [black arrows]). Reflectance measurements in nanowatts obtained with dual-fiberoptic probe (lower portion of graph) (see *Methods*). In this example, the optical trigger (vertical blue line) occurs 31 minutes prior to reaching the pathologically increased ICP of 20 mm Hg. *Left inset:* Baseline ICP waveform with low (< 5 mm Hg) variability. *Right inset:* Intracranial pressure waveform at higher pressure with increased amplitude of variability (> 5 mm Hg) compared with baseline ICP. **B:** Intracranial pressure recordings (upper portion of graph) before and after the injection of normal saline (30% body weight, intraperitoneally; black arrows). The reflectance measured in nanowatts (lower portion of graph) obtained with dual fiberoptic probe. In this example, the ICP recording shows a steady baseline unaltered by normal saline injection. Also, the reflectance remains stable throughout the length of the experiment. **C:** Time interval between water injection (Time Point 0), optical trigger, and defined threshold ICP values (3 mice; mean \pm SEM). The optical trigger (double asterisks) is detected significantly earlier than any of the ICP thresholds ($p < 0.001$). **D:** Relationship of look-ahead distance to laser diode power using a solid-liquid interface. Laser diode power was linearly related to the look-ahead distance (as defined in *Methods*).

ther studies could evaluate other single-wavelength NIR laser diodes for comparison.

The main advantages of our optical approach are that cerebral edema can be detected early in a real-time and minimally invasive manner. This may allow for earlier initiation of appropriate treatments, such as hyperosmolar therapy.² Therefore, our NIR probe may prove to be a unique diagnostic tool in a variety of disease states associated with cerebral edema. For example, cerebral ischemia results in cytotoxic edema (with a contribution from vasogenic edema hours to days later secondary to endothelial cell dysfunction).^{7,21,25} Therefore, as it detects cytotoxic edema, our system may prove to be a sensitive detector of early cerebral ischemia. Another important clinical problem is traumatic brain injury and posttraumatic edema, in

which cytotoxic edema is thought to predominate.¹¹ Fiberoptic NIR monitoring may provide a timely warning of stroke or traumatic brain injury, obviating the need to wait for a clinical suspicion to develop prior to the consideration of appropriate diagnostic tests and interventions.

Conclusions

In summary, we have validated a dual-fiberoptic NIR probe in the early identification of cerebral edema before increases in ICP. The power of fiberoptic NIR detection lies in its ability to assess brain tissue directly without relying on late changes in ICP. This technique will need to be validated in other models of cerebral edema—for example, traumatic brain injury and ischemia. Conceivably, sensitive

optical detection of focal changes in NIR reflectance could serve as a powerful early diagnostic tool in diverse disease states.

Disclosure

This work was supported by an American Association of Neurological Surgeons Medical Student Summer Research Fellowship (A.S.G.), postgraduate research fellowships from UCI (K.F.R., C.M.O.), and a Mentored Clinical Scientist Research Career Development Award (NIH K08 NS059674) (D.K.B.). The authors are indebted to Alan Verkman for the provision of the AQP4^{-/-} mice used in these studies, and to Sophie Chung at the Beckman Laser Institute, UCI for use of FDP equipment. All ongoing studies are being carried out using protocols approved by UCI's Institutional Animal Care and Use Committee.

Author contributions to the study and manuscript preparation include the following. Conception and design: DK Binder. Acquisition of data: AS Gill, KF Rajneesh, CM Owen, JJ Yeh. Analysis and interpretation of data: DK Binder, AS Gill, KF Rajneesh. Drafting the article: AS Gill, KF Rajneesh. Critically revising the article: DK Binder. Reviewed final version of the manuscript and approved it for submission: DK Binder, AS Gill, KF Rajneesh, CM Owen, JJ Yeh, MS Hsu. Statistical analysis: KF Rajneesh. Administrative/technical/material support: DK Binder, MS Hsu. Study supervision: DK Binder.

References

- Attas M, Hewko M, Payette J, Posthumus T, Sowa M, Mantsch H: Visualization of cutaneous hemoglobin oxygenation and skin hydration using near-infrared spectroscopic imaging. **Skin Res Technol** 7:238–245, 2001
- Bratton SL, Chestnut RM, Ghajar J, McConnell Hammond FF, Harris OA, Hartl R, et al: Guidelines for the management of severe traumatic brain injury. II. Hyperosmolar therapy. **J Neurotrauma** 24 (Suppl 1):S14–S20, 2007
- Czosnyka M, Pickard JD: Monitoring and interpretation of intracranial pressure. **J Neurol Neurosurg Psychiatry** 75:813–821, 2004
- Dawson JB, Barker DJ, Ellis DJ, Grassam E, Cotterill JA, Fisher GW, et al: A theoretical and experimental study of light absorption and scattering by in vivo skin. **Phys Med Biol** 25:695–709, 1980
- Emerson MR, Nelson SR, Samson FE, Pazdernik TL: A global hypoxia preconditioning model: neuroprotection against seizure-induced specific gravity changes (edema) and brain damage in rats. **Brain Res Brain Res Protoc** 4:360–366, 1999
- Hale GM, Querry MR: Optical constants of water in the 200-nm to 200- μ m wavelength region. **Appl Opt** 12:555–563, 1973
- Heo JH, Han SW, Lee SK: Free radicals as triggers of brain edema formation after stroke. **Free Radic Biol Med** 39:51–70, 2005
- Johns M, Giller CA, German DC, Liu H: Determination of reduced scattering coefficient of biological tissue from a needle-like probe. **Opt Express** 13:4828–4842, 2005
- Ma T, Yang B, Gillespie A, Carlson EJ, Epstein CJ, Verkman AS: Generation and phenotype of a transgenic knockout mouse lacking the mercurial-insensitive water channel aquaporin-4. **J Clin Invest** 100:957–962, 1997
- Manley GT, Fujimura M, Ma T, Noshita N, Filiz F, Bollen AW, et al: Aquaporin-4 deletion in mice reduces brain edema after acute water intoxication and ischemic stroke. **Nat Med** 6:159–163, 2000
- Marmarou A: Pathophysiology of traumatic brain edema: current concepts. **Acta Neurochir Suppl** 86:7–10, 2003
- Marmarou A, Poll W, Shulman K, Bhagavan H: A simple gravimetric technique for measurement of cerebral edema. **J Neurosurg** 49:530–537, 1978
- Mourant JR, Freyer JP, Hielscher AH, Eick AA, Shen D, Johnson TM: Mechanisms of light scattering from biological cells relevant to noninvasive optical-tissue diagnostics. **Appl Opt** 37:3586–3593, 1998
- Nakajima R, Nakamura T, Ogawa M, Miyakawa H, Kudo Y: Novel method for quantification of brain cell swelling in rat hippocampal slices. **J Neurosci Res** 76:723–733, 2004
- Nelson SR, Mantz ML, Maxwell JA: Use of specific gravity in the measurement of cerebral edema. **J Appl Physiol** 30:268–271, 1971
- Park E, Bell JD, Baker AJ: Traumatic brain injury: can the consequences be stopped? **CMAJ** 178:1163–1170, 2008
- Piao D, Pogue BW: Rapid near-infrared diffuse tomography for hemodynamic imaging using a low-coherence wideband light source. **J Biomed Opt** 12:014016, 2007
- Qian Z, Victor S, Gu Y, Giller C, Liu H: Look-Ahead Distance of a fiber probe used to assist neurosurgery: phantom and Monte Carlo study. **Opt Express** 11:1844–1855, 2003
- Rasmussen P, Dawson EA, Nybo L, van Lieshout JJ, Secher NH, Gjedde A: Capillary-oxygenation-level-dependent near-infrared spectrometry in frontal lobe of humans. **J Cereb Blood Flow Metab** 27:1082–1093, 2007
- Rolfe P: In vivo near-infrared spectroscopy. **Annu Rev Biomed Eng** 2:715–754, 2000
- Rosenberg GA: Ischemic brain edema. **Prog Cardiovasc Dis** 42:209–216, 1999
- Schmitt JM, Kumar G: Optical scattering properties of soft tissue: a discrete particle model. **Appl Opt** 37:2788–2797, 1998
- Suzuki S, Takasaki S, Ozaki T, Kobayashi Y: A tissue oxygenation monitor using NIR spatially resolved spectroscopy. **SPIE** 3597:582–592, 1999
- Thiagarajah JR, Papadopoulos MC, Verkman AS: Noninvasive early detection of brain edema in mice by near-infrared light scattering. **J Neurosci Res** 80:293–299, 2005
- van Gelderen P, de Vleeschouwer MH, DesPres D, Pekar J, van Zijl PC, Moonen CT: Water diffusion and acute stroke. **Magn Reson Med** 31:154–163, 1994
- Verkman AS, Binder DK, Bloch O, Auguste K, Papadopoulos MC: Three distinct roles of aquaporin-4 in brain function revealed by knockout mice. **Biochim Biophys Acta** 1758:1085–1093, 2006
- Weast RC (ed): **Handbook of Chemistry and Physics**, ed 57. Cleveland, OH: Chemical Rubber, 1976
- Wilson JD, Bigelow CE, Calkins DJ, Foster TH: Light scattering from intact cells reports oxidative-stress-induced mitochondrial swelling. **Biophys J** 88:2929–2938, 2005

Manuscript submitted August 17, 2009.

Accepted February 3, 2010.

Please include this information when citing this paper: published online March 5, 2010; DOI: 10.3171/2010.2.JNS091017.

Address correspondence to: Devin K. Binder, M.D., Ph.D., Center for Glial-Neuronal Interactions, Division of Biomedical Sciences, University of California, Riverside, California. email: dbinder@ucr.edu.